Tellus (1989), *41A*, 308–318

Objective mesoscale analysis of daily extreme temperatures in the Po Valley of northern Italy

By CARLO CACCIAMANI, TIZIANA PACCAGNELLA, SANDRO NANNI,
Regional Meteorological Service of Emilia-Romagna, Via S. Felice 25, 40122 Bologna, Italy
and STEFANO TIBALDI*, *ECMWF, Shinfield Park, Reading RG2 9AX, UK*

(Manuscript received 23 December 1987; in final form 23 September 1988)

ABSTRACT

In this paper, an optimum interpolation scheme is applied to produce an objective daily mesoscale analysis of minimum and maximum temperatures in the Emilia Romagna region of northern Italy (essentially the Po Valley). This system is operational at the Regional Meteorological Service. The study of the autocorrelation structures of these fields shows the strong anisotropy induced by the morphological characteristics of the region, and particularly by the Apennines and the Adriatic Sea. To evaluate the structure functions, a data set of the National Hydrological Service has been used. The data, from 1961 to 1977, are available in about 40 stations covering the region fairly uniformly. The analysis scheme is univariate and the structure functions have been evaluated separately for every month of the year.

1. Introduction

The objective analysis of a meteorological parameter consists in spreading the available information, relative to a certain number of points irregularly distributed within a certain area (the observation points), to other points of the same area (the analysis points, usually regularly spaced) in which the information is not directly available. This operation has to be performed so as to determine a meteorological field in which observations are represented satisfactorily and the spatial structures of interest correctly reproduced (for a general review see, for example, Creutin and Obled, 1982).

Several objective analysis schemes compute the analysed value on the basis of both observations and a first guess field (FG), determined a priori both at the stations points and at the analysis points. If A_k^{an} is the analysed value at point k, A_k^p is the FG at that point, and A_j^o and A_j^p are the observation and FG at the jth station, the general relationship at the basis of such analysis schemes is (see the Appendix for symbols):

$$A_k^{an} - A_k^p = \sum_{j=1}^{N} W_{kj}(A_j^o - A_j^p), \tag{1}$$

with $k = 1, 2, \ldots M$; M is the number of points over which the analysis is performed; N is the number of observations used to compute the analysed value at point k and W_{kj} is the relative weight of station j with respect to point k.

The general formulation based on eq. (1) depends crucially upon the choice of the first guess and of the weights W_{kj}. The optimum interpolation (OI) method (Eliassen, 1954 and Gandin, 1965) is a statistical analysis procedure in which the weights W_{kj} are determined from the knowledge of the autocorrelation field of the parameter. In this work we have applied the OI procedure to the objective analysis of daily minimum (T_{min}) and maximum (T_{max}) temperature fields over the Italian region of Emilia Romagna (this region covers most of the Po Valley area, in northern Italy).

In Section 2 we describe the data and the region's morphology. Section 3 briefly recalls some relevant theoretical aspects of the OI

* Current affiliation: University of Bologna, Dept. of Physics, Via Irnerio 46, 40126 Bologna, Italy.

method, Section 4 describes the field structure functions derived from the historical data set, while Section 5 discusses the choice of the FG field, Section 6 describes the results of the analysis procedure and Section 7 contains some conclusions.

2. The geography of the Emilia Romagna region and the station network

The Emilia Romagna region (ER) lies in the south-east part of the Po Valley, in northern Italy, and is bounded by the Adriatic Sea to the east and by the Apennine mountain range to the south and south-west. The total area of the region is approximately 23 000 km^2. It is mainly flat in the northern part, while the terrain raises steeply towards the south-west where mountain peaks higher than 2000 m are to be found. Fig. 1 shows the region under study, its orography (obtained from the US Navy high resolution topography dataset) and the location of the weather stations. A historical data set of minimum and maximum daily temperatures measured in about 40 stations of fairly homogeneous distribution throughout the area is available and was used to evaluate the structure functions used in the OI analysis.

At present, temperature measurements from nine synoptic stations of the National Weather Service and six automatic stations of the Regional Meteorological Service (SMR) of Emilia Romagna are available in real time to the forecasting branch of SMR (and are also included in the World Weather Watch). The above network of stations provides real time data for analysis using the scheme proposed in this paper.

3. Some theoretical aspects of optimum interpolation

Eq. (1) can be rewritten, using the notations given in the Appendix, as:

$$a_k = p_k + \sum_{j=1}^{N} W_{kj} b_j. \tag{2}$$

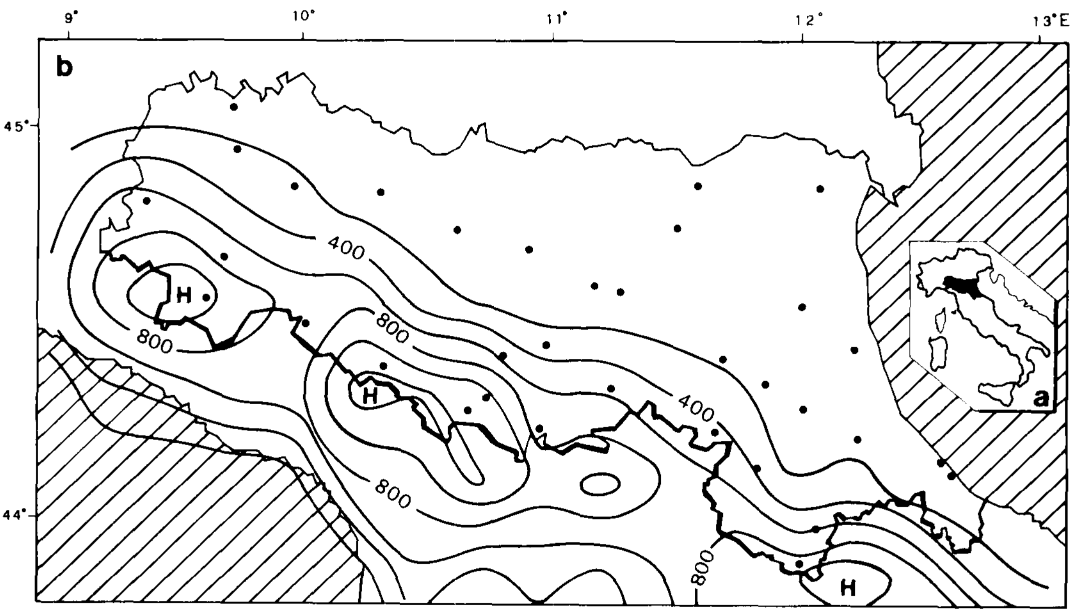

Fig. 1. (a) Location map of Emilia Romagna region. (b) Schematic map of the orography of the Emilia Romagna as deduced from the US Navy high-resolution topography (isolines every 200 m). The dotted circles represent the meteorological stations of the National Hydrological Service.

The OI technique allows to estimate the weights W_{kj} by minimising the squared analysis error $\langle a_k^2 \rangle$, averaged over a large ensemble of analyses. By squaring eq. (2) and averaging over the ensemble, one obtains:

$$\langle a_k^2 \rangle = \langle p_k^2 \rangle + \sum_{j=1}^{N} \sum_{l=1}^{N} W_{kj} W_{kl} \langle b_j b_l \rangle + 2 \sum_{j=1}^{N} W_{kj} \langle p_k b_j \rangle. \quad (3)$$

We observe that, in the hypothesis that $\langle p_k o_j \rangle = 0$, i.e., that there is no correlation between observation error and first guess error in different points, we get $\langle p_k b_j \rangle = -\langle p_k p_j \rangle$. Then eq. (3) becomes:

$$\langle a_k^2 \rangle = \langle p_k^2 \rangle + \sum_{j=1}^{N} \sum_{l=1}^{N} W_{kj} W_{kl} \langle b_j b_l \rangle - 2 \sum_{j=1}^{N} W_{kj} \langle p_k p_j \rangle. \quad (4)$$

By imposing the minimisation condition:

$$\frac{\partial \langle a_k^2 \rangle}{\partial W_{ki}} = 0 \quad (i = 1, 2, \ldots N), \quad (5)$$

we obtain, for each point k a system of N linear equations:

$$\sum_{j=1}^{N} W_{kj} \langle b_j b_i \rangle = \langle p_k p_i \rangle \quad (i = 1, 2, \ldots N), \quad (6)$$

and observing that (remembering again that $\langle o_j p_i \rangle = 0$)

$$\langle b_j b_i \rangle = \langle p_j p_i \rangle + \langle o_j o_i \rangle, \quad (7)$$

system (6) becomes:

$$\sum_{j=1}^{N} W_{kj} (\langle p_j p_i \rangle + \langle o_j o_i \rangle) = \langle p_k p_i \rangle. \quad (8)$$

Using matrix notation:

$$W = W_{kj}, \quad B = \langle p_i p_j \rangle + \langle o_i o_j \rangle, \quad D = \langle p_k p_i \rangle,$$

eq. (7) can be rewritten in matrix form as:

$$W \cdot B = D \quad (9)$$

so that the weight matrix is easily obtained:

$$W = D \cdot B^{-1}. \quad (10)$$

4. Determination of the structure functions

The solution of eq. (10) is dependent upon the knowledge of the matrices B and D and upon the knowledge of the covariance matrices $\langle p_i p_j \rangle$ (first guess error covariance matrix) and $\langle o_i o_j \rangle$ (observation error covariance matrix). The $\langle p_i p_j \rangle$ and $\langle o_i o_j \rangle$ matrices cannot be evaluated because the true field is not known; the B matrix is known (in principle) because it is the sum of first guess error and observational error covariance matrices, but can, in practice, be ill conditioned (due to inaccuracies in the computation or to inadequacies of the observational network) and cause problems during inversion. These problems can be overcome by parameterizing $\langle p_i p_j \rangle$ and $\langle o_i o_j \rangle$ (e.g., Thiebaux, 1975).

In line with Schlatter et al. (1976), we assume that the observational errors are uncorrelated and so $\langle o_i o_j \rangle = O^2 \cdot \delta_{ij}$, where O^2 is the observational error variance. Then equation (7) becomes:

$$\langle b_i b_j \rangle = \langle p_i p_j \rangle + O^2 \delta_{ij}.$$

If $i \neq j$ (non-coincident stations), the first guess covariance matrix is equal to the total error covariance matrix; if $i = j$ we must add the observational error variance at point i (j) to the first guess variance to obtain the total error variance. According to this, we define the first guess covariance matrix $\langle p_i p_j \rangle$ as:

$$\langle p_i p_j \rangle \equiv \langle b_i b_j \rangle = \mu_{ij} \Gamma_i \Gamma_j \quad \text{if } i \neq j$$

$$\langle p_i p_i \rangle = \Gamma_i^2 - O^2 \quad \text{if } i = j;$$

therefore

$$\langle b_i b_i \rangle = \Gamma_i^2$$

and

$$\mu_{ij} = \frac{\langle b_i b_j \rangle}{\Gamma_i \Gamma_j} \quad \text{with } i \neq j$$

$$\mu_{ii} = 1 - \frac{O^2}{\Gamma_i \Gamma_i}.$$

The normalized first guess covariance μ is generally modelled using some analytical function $F(v_1, v_2, \ldots, a_1, a_2, \ldots)$, where v_1, $v_2 \ldots$ are geometric or geographic parameters and a_1, a_2, ... are coefficients evaluated by fitting the observed correlation matrix.

When applying the OI technique on the synoptic scale, the autocorrelation field is usually taken

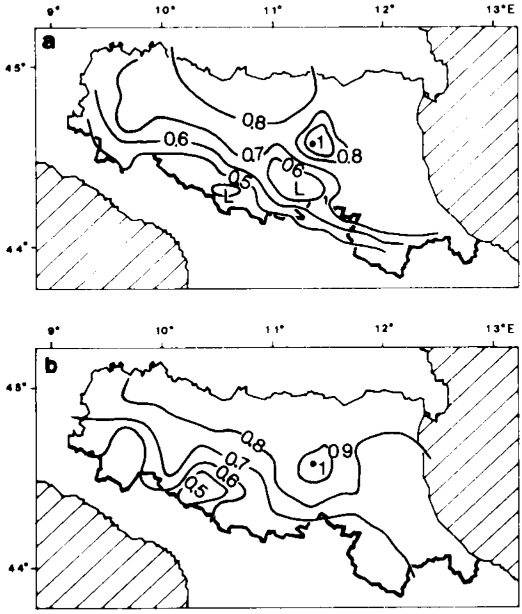

Fig. 2. Monthly mean correlation of minimum temperature between Bologna (base point, indicated by a dot) and surrounding stations: (a) January and (b) July. Isolines every 0.1.

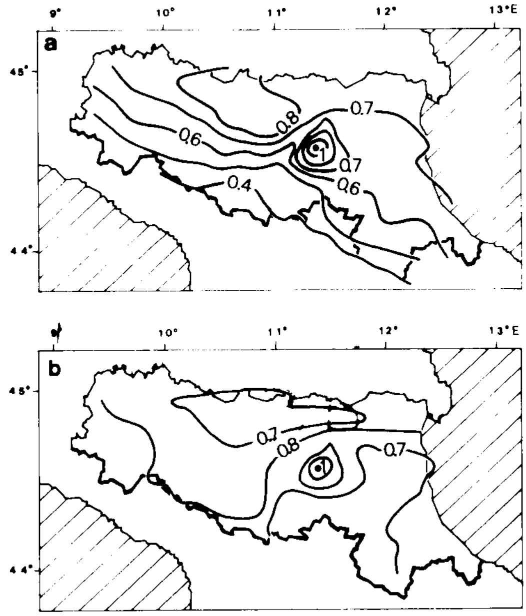

Fig. 3. As in Fig. 2, but for maximum temperature.

to be isotropic and homogeneous and functions $F = F(r_{ij})$ are used where r_{ij} is the distance between point i and point j. Such hypotheses are no longer appropriate on smaller scales (especially when analysing parameters at ground level, therefore closely related to the morphological features of the region), Thiebaux (1976 and 1977), Seaman and Gauntlett (1980), Buell and Seaman (1983) and Gustafsson (1985). In Fig. 2 the correlation of the minimum temperature between the Bologna station and the other stations of the region is shown respectively for the months of January, and July. In Fig. 3, the same is shown for maximum temperature. It can be seen how the topography of the region induces a strong anisotropy in the correlation which has an almost elliptical symmetry with the major axis parallel to the Apennines. The correlation drop due to station height differences is also evident.

In Figs. 4, 5, scatter diagrams are shown for the correlation, relative to minimum temperature, between each pair of stations against their relative distance for the months of January and August respectively. In panels (b) of the figures, the correlations between all pairs of stations are reported, while in panels (a) only those pairs of stations with a relative elevation difference less than 500 m are shown. Here we can see both how the correlation decreases with increasing horizontal distance and also the pronounced effect produced by differences in elevation, especially in January. From panel (a) it is seen how the correlation never falls below 0.6 if stations with large height differences are excluded. On the contrary, considering all stations, values of correlation of about 0.4 even for very short horizontal distances between stations (100–150 km) are possible. It would then be inappropriate to suppose that the correlation field is isotropic and thus use structure functions with a radial symmetry.

For example, Gustafsson (1985), in estimating mesoscale structure functions for temperature and relative humidity at ground level, deals with the problem of anisotropy by classifying the stations on the basis of their geographic location and associating different weights to each station according to its class. From the results of the discussion above, it was decided to account for correlation anisotropy by defining a two variable structure function (horizontal distance and elev-

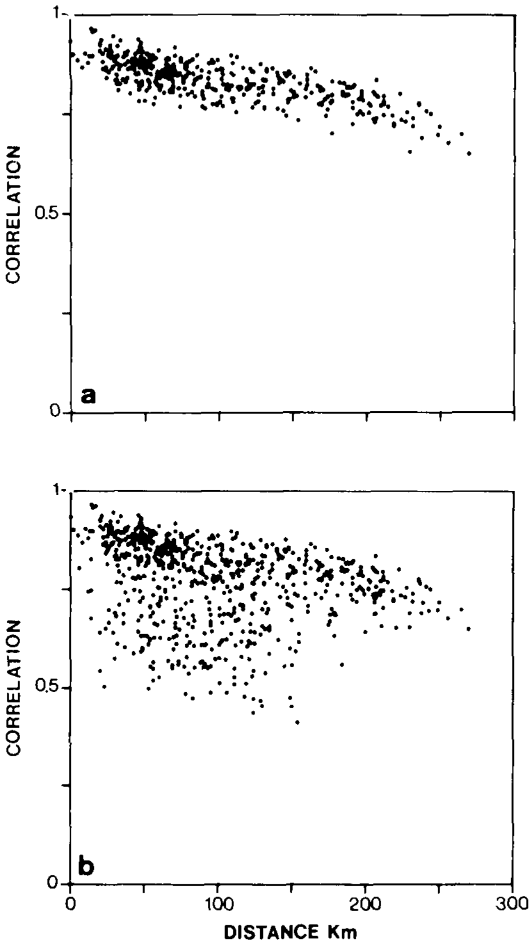

Fig. 4. Scatter diagrams of minimum temperature correlation between each pair of stations against their relative distance for the month of January: (a) only stations with a relative height difference smaller than 500 m are included; (b) all stations.

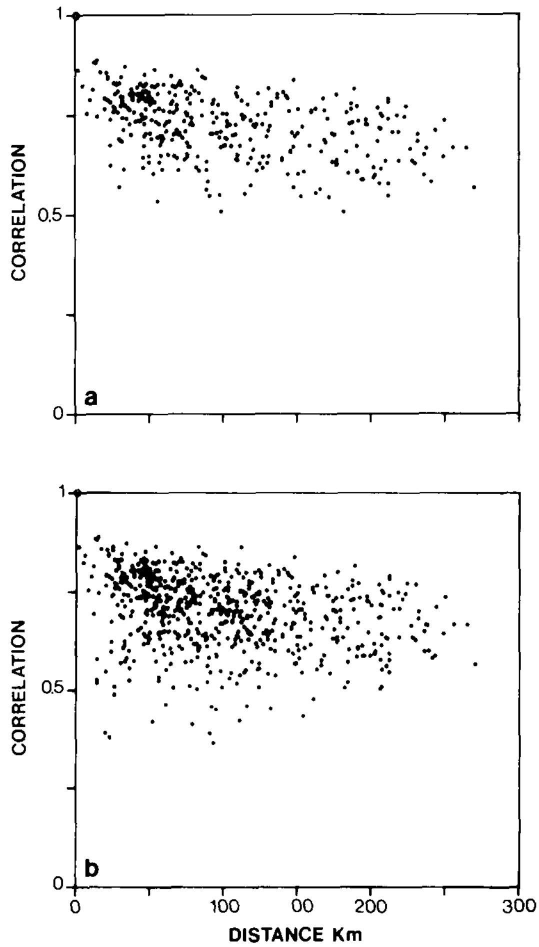

Fig. 5. As in Fig. 4, but for the month of August.

ation difference). From Figs. 2 to 5, the month-to-month variability of the correlation structure is also evident and, therefore, separate structure functions have been computed for each month of the year.

To evaluate the impact of this approach, two different least square best-fits of the correlation data were performed using the two following structure functions:

$$F_1^m(r_{ij}) = A^m \exp(B^m \cdot r_{ij}),$$

$$F_2^m(r_{ij}, |dz_{ij}|) = A^m \exp(B^m \cdot r_{ij}) \exp(C^m \cdot |dz_{ij}|),$$

where r_{ij} is the distance between stations i and j and $|dz_{ij}|$ is the absolute value of the elevation difference between stations i and j; A, B and C are the best-fit coefficients, and $m = 1, \ldots, 12$ is the month index.

In Figs. 6a and 6b, the correlation field of January minimum temperature between the Piacenza station (situated in the north-west part of the region) and the surrounding stations has been modelled with functions F_2 and F_1 respectively. Fig. 6c shows the corresponding observed field, for the same month. The structure of the observed field shows a strong effect of the Adriatic sea in the eastern part of the region and the effect of the Apennines in the southern part,

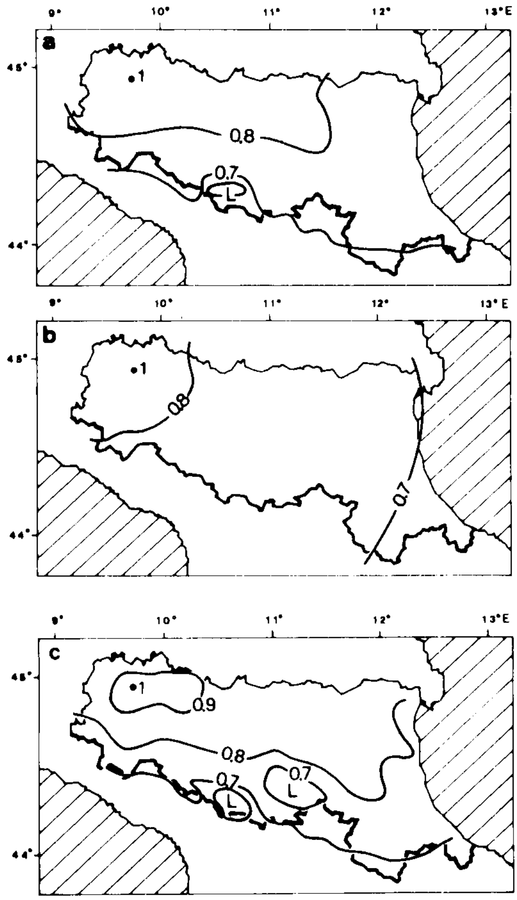

Fig. 6. Correlation field of minimum temperature between Piacenza (base point, marked with a dot) modelled with functions F_2 (a) and F_1 (b). Panel (c) contains observed values for the same month of January. Isolines every 0.1.

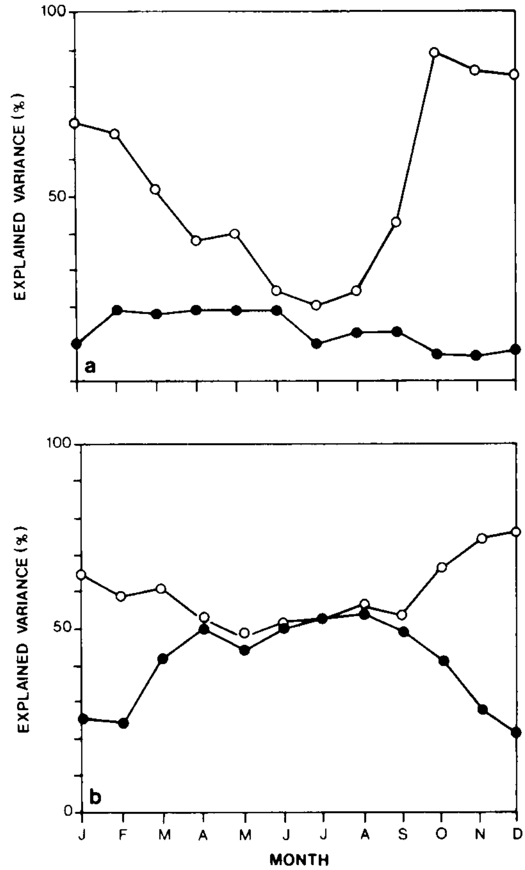

Fig. 7. Proportion of explained variance (PEV) by the two analytical structure functions F_1 (closed circles) and F_2 (open circles) for each month of the year: (a) minimum temperature; (b) maximum temperature.

while in the north-western part of the Po Valley the correlation tends to be almost constant with longitude.

By comparing the three panels of Fig. 6, it can be noted how the observed elliptical structure (with the major axis parallel to the Apennines) is well captured by F_2, but not by F_1. It can however also be seen how F_2 provides a fair representation of only one of the two observed minima of Fig. 6c, the one corresponding to the maximum of the topography (see Fig. 1). On the contrary, F_1 is completely unable to represent any structure.

In Fig. 7 the proportion of explained variance (PEV) by F_1 and F_2 is shown as a function of the month of the year for both variables T_{min} and T_{max}. F_2 has larger values of PEV, compared to F_1, for every month of the year for both T_{min} and T_{max}, and particularly so during the colder period (October to March), while the improvement over F_1 is moderate during the warmer period (April to September).

Examining the curves relative to the minimum temperature (Fig. 7a) it can be seen how the F_1 PEV is almost constant throughout the year, ranging from 7% to 20%, while the F_2 PEV shows a larger variability, ranging from 20% in

July to 90% in October with a rapid transition from summer to winter. The same behaviour is seen for the maximum temperature with a less sharp transition from summer to winter.

For both T_{min} and T_{max} two main types of climatological regime are evident: a winter type, during which the difference in station elevation is crucial in determining the main structure of the correlation field, and a summer type during which the importance of station elevation decreases practically to zero, especially for the maximum temperature.

Furthermore, it is important to note how the PEV relative to F_1 and F_2 has opposite trends during the winter. The F_1 PEV increases from January to April and decreases from August to December, while the F_2 PEV behaves oppositely. This can be interpreted remembering that, during winter, when the influence of the large-scale circulation dominates over local effects, the lower troposphere is often stably stratified due to the presence of strong thermal inversions that prevent vertical mixing. Under such conditions, two stations located not far from each other in the horizontal but at different heights belong to air masses of different thermodynamic characteristics, making the variation in height an important parameter in the structure function.

During summer, strong surface inversions are extremely rare and the circulation in the Po Valley is mainly driven by local mechanical and thermal effects, since large-scale synoptic forcing is much weaker: the Planetary Boundary Layer (PBL) over the Po Valley is therefore characterized by a strong vertical mixing with a general weakening of vertical stability. The relative distance between the stations becomes then the main factor, while the effect of the elevation difference is much less important. On the basis of these results, F_2 was chosen as the functional form for the structure function.

In Fig. 8 the values of the coefficients A, $1/B$ and $1/C$ of F_2, are shown as functions of the months of the year for T_{min} and T_{max}. In agreement with the results just presented, the difference in height is again important only during the winter period. The vertical length scale F_2, $1/C$, is very large, especially for T_{max}, during the summer months. On the contrary, the horizontal length scale $1/B$ shows a maximum during the winter months with a general decrease, with some oscillations, during the summer period.

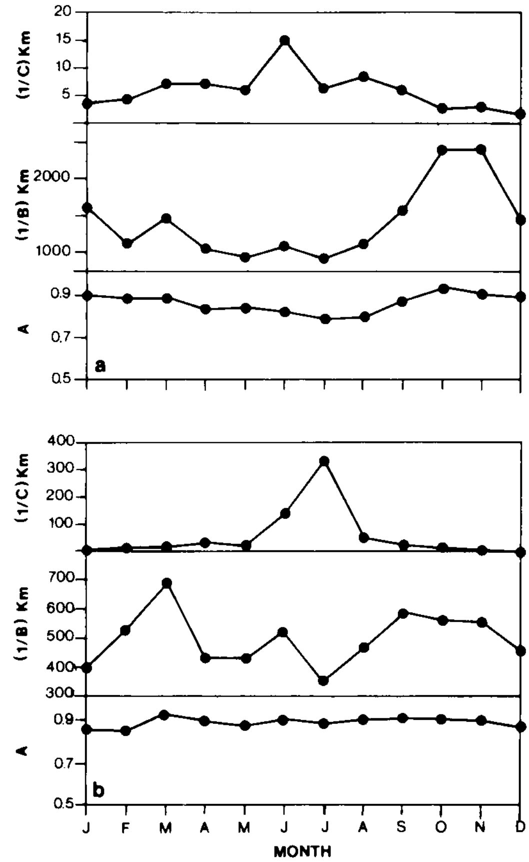

Fig. 8. Values of the F_2 structure function coefficients $1/C$ (top graph), $1/B$ (middle graph) and A (lower graph) as functions of the month of the year: (a) minimum temperature, (b) maximum temperature.

To evaluate the observational error variance O^2 we used the relation (Gandin, 1965):

$$O^2 = (1 - A)\Gamma^2,$$

where A is the intercept of the structure function F_2 when both the horizontal distance and the elevation difference tend to zero.

5. The choice of the first guess

The performance of any objective analysis scheme, as pointed out earlier, depends heavily on the choice of the first guess field. The usual

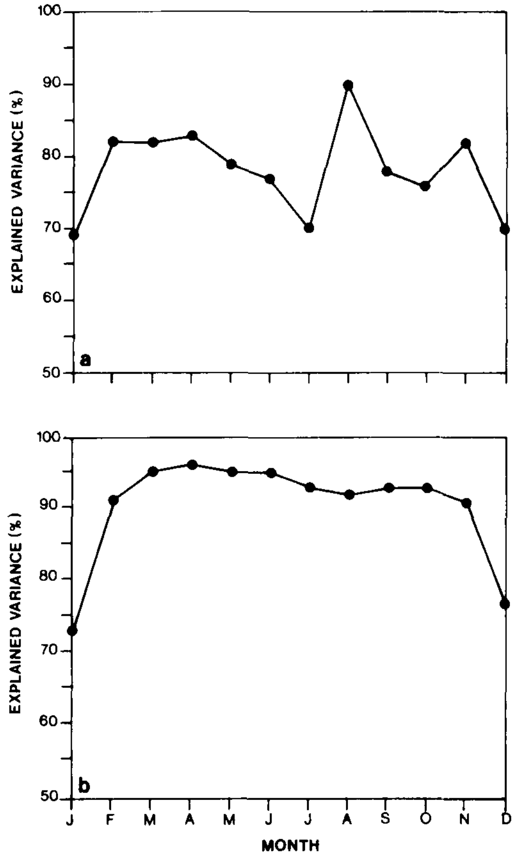

Fig. 9. Proportion of explained variance (PEV) as a function of the month of the year attained by defining climatology with the linear regression model: (a) minimum temperature, (b) maximum temperature.

possible alternatives for the FG field are climatology, persistence, an analysis at a coarser resolution or the output of a numerical weather prediction model (a short-range forecast for the situation to be analysed). We decided to use monthly climatology as the first guess field.

This choice became necessary, on one hand, because no short-range forecast of near-surface temperature extrema from a mesoscale numerical model or a larger scale analysis is operationally available; on the other hand, persistence caused problems in data void areas. (Work to use damped persistence following Schlatter, 1975, is however in progress.) Furthermore, as Cats (1980) points out, the use of climatology has the advantage of making the analysis procedure independent from the characteristics of the model from which the FG could possibly be derived.

From eq. (1), it is evident how the FG has to be known both at observation points and at analysis points. Following Cats (1980), the FG was analytically defined as a best-fitted function of longitude (that in our particular situation models the distance from the sea) and station height, for T_{min}, and also on latitude for T_{max}. In view of the limited size of the region considered, a linear fitting was considered appropriate. Including latitude as a best fit parameter for T_{max} resulted in an appreciable increase in the proportion of explained variance. On the other hand, the improvement was negligible for T_{min}. Fig. 9 shows the monthly PEV attained by defining the climatology of T_{min} and T_{max} using this linear regression. For maximum temperature, the values are very high, except for January and December, supporting the hypothesis that (with the exception of winter) local effects dominate over large-scale dynamics. The relatively low values during the cold period suggest that it could be useful to introduce more information in the regression equation on the nature of the air mass.

To actually perform an analysis, it is also necessary to evaluate the climatological standard deviation of the analysed parameters. Since no obvious functional relationship between standard deviation of T_{min} and T_{max} and geographical parameters was found, this was obtained at analysis points from a simple distance-weighted interpolation from observed stations point values.

6. Discussion of the results

To test the overall performance of the analysis procedure, daily objective analyses of minimum and maximum temperature for the period 1961–1977, using monthly varying structure function parameters and climatological first guess were performed. Six stations were excluded to provide a minimal database to compute independently the root mean square (RMS) departure of the analysis from observations, i.e.:

$$\text{RMS error} = \overline{(\langle(\text{observation} - \text{analysed value})^2\rangle^{1/2})},$$

where the overbar indicates the ensemble value over the six stations excluded from the analysis

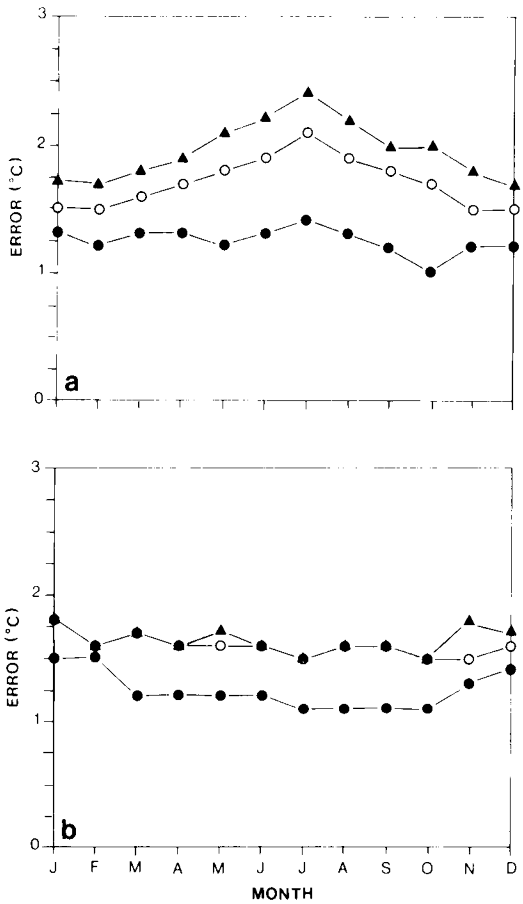

Fig. 10. Observational error O (full circles), RMS analysis minus observation departure for the LR experiment (triangles) and for the HR experiment (open circles): (a) minimum temperature, (b) maximum temperature.

procedure. This RMS departure can be compared with the estimated observational variance O^2, also averaged over the six stations.

We performed the entire analysis procedure twice, in order to test the sensitivity of the method to the number of stations used and therefore to the resolution of the observational network. The first time the whole dataset, including about 30 stations was used (High-Resolution experiment, HR). The second time, only 18 stations were used (Low-Resolution experiment, LR), thereby approximately reproducing the geographic distribution of the regional weather service operational network.

Regarding the OI definition of the observational error, we used the value of A and Γ derived from the structure functions computed using the complete data set (37 stations), after having observed that it depends little upon the total number of stations used. In Fig. 10, the monthly values of observational error O and of analysis minus observation RMS departure are shown for both high and low resolution experiments. Panel (a) refers to T_{min} and panel (b) to T_{max}. From panel (a) we can see how the RMS departure for the HR experiment is always lower than for the LR experiment. It ranges from 1.5°C in January to 2.2°C in July. This improvement in the T_{min} HR experiment underlines the micro-scale nature of this particular parameter. The average difference between O and RMS departure (to be interpreted as an estimate of the analysis error) is around 0.3° for the HR experiment and shows a maximum value around 0.6° in correspondence to the summer months. From panel (b), we observe some important differences in the behaviour of the T_{max} analysis with respect to the T_{min} analysis. Firstly, there is no evidence of a measurable improvement in the HR experiment in comparison with the LR. Another difference is the decrease of the seasonal dependency of the RMS error. The general worsening of results obtained during summer time (much more evident for T_{min}) is most linked to micro-scale phenomena which tend to reduce the autocorrelation of the ground level thermal field. Such a result is consistent with the decreased fit of the F_2 structure function to the observed data during summer time. More work is needed to introduce, during summer, information of a microclimatic nature for a better description of the thermal field.

7. Conclusions

In this paper, we have analysed the performance of an Optimum Interpolation analysis scheme of surface temperature extrema in the Emilia Romagna region of northern Italy. To define the appropriate structure functions we have studied the spatial structure of the autocorrelation fields of maximum and minimum temperature. Monthly climatology has been used as first guess field. The historical data set used to evaluate the structure functions and test the analysis procedure was obtained from about 40 weather stations of the National Hydrological Service covering the period 1961–1977.

We have then applied the daily analysis procedure to the whole data set but excluding six stations that we have used to test the performance of the procedure. Several conclusions have emerged regarding the structure functions, the climatology of temperature extrema and the results obtained with the analysis system described.

(1) Anisotropy is an important factor in defining the structure functions of near-surface temperature extrema. We attempted to improve the analytical model of the autocorrelation field by introducing the absolute value of height difference between stations as the anisotropy element. The improvement is considerable during winter, but absent during summer.

(2) The structure functions coefficients show a strong seasonal dependence.

(3) The climatological structures of near-surface temperature extrema in the Po Valley are heavily influenced by the presence of the (complex) surrounding orography and of the Adriatic Sea. In using climatology as a First Guess field, it is possible to take into account some of these effects by incorporating a linear dependency upon local geographical parameters, i.e., station height, latitude and longitude. This parameterization is very successful during the warm season (April–September), but much less satisfactory during winter time when the influence of synoptic and sub-synoptic scale circulation system (e.g., cyclones, fronts) is dominant and requires a mesoscale-forecast-type First Guess field.

(4) The analyses produced are of better quality (as measured from RMS departure from independent observations) during winter than during summer.

(5) The effect of data density is different on maximum and minimum temperature; when a denser observational network is used noticeable improvements are observed only on the analysis of minimum temperature but not of maximum temperature. These improvements show no appreciable seasonal dependency.

8. Acknowledgements

We are indebted to Dr. P. Lonnberg of ECMWF, Reading, UK, for having read carefully an early version of the manuscript and for suggesting several points of clarification. We thank Dr. F. Tampieri of CNR-FISBAT, Bologna, Italy, for very useful discussions. We also thank the anonymous referees for many valuable recommendations.

9. Appendix

$\langle\ \rangle$	indicates ensemble mean.

By index k we identify analysis points, by indices i and j observation points.

$A^{t}_{k(j)}$	true field at point $k(j)$
A^{an}_{k}	analysed field at point k
A^{p}_{k}	first guess (FG) field at point k
A^{o}_{j}	observed field at point j
A^{p}_{j}	first guess field at point j
$b_j = A^{o}_{j} - A^{p}_{j}$	observation–first guess departure
$o_j = A^{o}_{j} - A^{t}_{j}$	observation–true field departure
$p_j = A^{p}_{j} - A^{t}_{j}$	first guess–true field departure
$a_k = A^{an}_{k} - A^{t}_{k}$	analysis–true field departure
$\Gamma_j = \langle b_j b_j \rangle^{1/2}$	total error
$O_j = \langle o_j o_j \rangle^{1/2}$	observational error
$P_j = \langle p_j p_j \rangle^{1/2}$	first guess error

We observe that:

$$\Gamma_j^2 = O_j^2 + P_j^2, \quad \text{if } \langle o_j p_j \rangle = 0.$$

The true field is a hypothetic field from which all errors connected with observational techniques and the noise introduced by small-scale phenomena unresolved by the analysis procedure have been removed (Eddy, 1964).

REFERENCES

Buell, C. E. and Seaman, R. S. 1983. The "scissors" effect: anisotropic and ageostrophic influences on wind correlation coefficients. *Aust. Met. Mag. 31*, 77–83.

Cats, G. J. 1980. Analysis of surface wind and its gradient in a mesoscale wind observation network. *Mon. Wea. Rev. 108*, 1100–1107.

Creutin, J. D. and Obled, C. 1982. Objective analysis and mapping techniques for rainfall fields. *Wat. Res. Rev. 18*, 413–431.

Eddy, A. 1964. The objective analysis of horizontal wind divergence field. *Q. J. Roy. Met. Soc. 90*, 440–490.

Eliassen, A. 1954. Provisional report on calculation of spatial covariance and autocorrelation of pressure field. Inst. Weath. and Climat. Res., Acad. Sci., Oslo, Report no. 5.

Gandin, L. S. 1965. Objective analysis of meteorological fields. Israel Program for Scientific Translation, Jerusalem.

Gustafsson, N. 1985. Development of mesoscale analysis scheme for nowcasting and very short range forecasting. *Proceedings from Workshop on High Resolution Analysis*, ECMWF, UK, 24–26.

Schlatter, T. W. 1975. Some experiments with a multivariate statistical objective analysis scheme. *Mon. Wea. Rev. 103*, 246–257.

Schlatter, T. W., Branstator, G. W. and Thiel, L. G. 1976. Testing a global multivariate statistical objective analysis scheme with observed data. *Mon. Wea. Rev. 104*, 765–783.

Seaman, R. S. and Gauntlett, F. S. 1980. Directional dependence of zonal and meridional wind correlation coefficients. *Aust. Met. Mag. 28*, 217–218.

Thiebaux, H. J. 1975. Experiments with correlation representation for objective analysis. *Mon. Wea. Rev. 103*, 617–627.

Thiebaux, H. J. 1976. Anisotropic correlation functions for objective analysis. *Mon. Wea. Rev. 104*, 994–1002.

Thiebaux, H. J. 1977. Extending estimation accuracy with anisotropic interpolation. *Mon. Wea. Rev. 105*, 691–699.